Sigma J Eng & Nat Sci 38 (3), 2020, 1463-1480

Sigma Journal of Engineering and Natural Sciences
Sigma Mühendislik ve Fen Bilimleri Dergisi

Research Article

THE EFFECT OF CONCRETE SLAB THICKNESS ON SEISMIC PERFORMANCE OF CONCRETE FACE SLAB OF CFR DAMS

Murat Emre KARTAL*[1]

[1]*Izmir Democracy University, Department of Civil Engineering, İZMİR;* ORCID: 0000-0003-3896-3438

Received: 26.04.2020 Revised: 13.06.2020 Accepted: 25.07.2020

ABSTRACT

Concrete-faced rockfill (CFR) dams are known as least-cost alternative of clayey core rockfill (CCR) dams. Although clayey core material is a natural choice, it can not be obtained from the environment of the project area continually. CFR dams have increasingly been constructed in many parts of the world because of high resistance to ground motions. As the new experiences regarding these dams have been acquired, design properties of concrete slabs are altered in the course of time. One of the main concerns of CFR dams is the seismic performance of concrete slab during an earthquake. Therefore, the effect of face slab thickness on seismic performance of concrete slab on a CFR dam is investigated in this study. Torul CFR dam is chosen for numerical applications. Five different slab thicknesses derived from the formulations preferred in the literature are taken into consideration. Dam-reservoir-foundation interaction system is modeled by the finite element method. Contact analysis is also integrated in finite element analyses using interface element in concrete slab-rockfill interface. Hydrodynamic effects of the reservoir water are considered by the Lagrangian approach. In the nonlinear time-history analyses, Drucker-Prager model is used for concrete slab and multi-linear kinematic hardening model is utilized for rockfill zones and foundation soil. 1992 Erzincan earthquake with peak ground acceleration of 0.515g recorded near the dam site is used in numerical analyses. Linear and nonlinear analyses are carried out for different face slab thicknesses. According to this study, the increase in face slab thickness clearly improves the seismic performance of the concrete slab on CFR dam.

Keywords: Concrete-faced rockfill dams, dam-reservoir-foundation interaction, Drucker-Prager model, interface element, Lagrangian approach, seismic performance.

1. INTRODUCTION

Concrete-faced rockfill (CFR) dams have been built in many parts of the world especially in last decades [1] because of their high resistance to strong ground motions. CFR dams have more advantages such as, full use of local embankment materials, simply construction, short construction duration. This type of dams is also known as the least-cost alternative of clayey core rockfill (CCR) dams for its lower construction cost. Besides, although clayey core material is a natural choice, it cannot be obtained from the environment of the project area continually [2].

The two of the most important agents in CFR dams are seismic performance [1-8] and seepage performance of the concrete slab. Even if concrete face slab does not cause to leak, it may be exposed to high tensile and compression stresses during earthquake. If the concrete slab

* Corresponding Author: e-mail: murat.kartal@idu.edu.tr, tel: (232) 260 10 01 / 417

covering upstream face of the rockfill cracks, water will leak into dam and the stability of the dam may diminish [9]. As the new experiences regarding these dams have been acquired, design properties of concrete slabs have been altered in the course of time. For this purpose, various slab thickness combinations have been employed in CFR dams in last decades.

Though CFR dams involve fluid-structure-foundation interaction problems, hydrodynamic pressures on concrete slab have not been taken into account in the preceding studies. However, hydrodynamic pressure ef fects on dynamic response of dams have been started to be researched in 1930's [10-20]. Additionally, hydrodynamic pressure on concrete slab of CFR dams has been paid attention by the researchers [21-25].

In this study, the effect of concrete slab thickness on seismic performance of a CFR dam is investigated. Torul CFR dam is selected for numerical analyses. Various slab thickness functions were selected from the literature to show the thickens effect. Dam-reservoir-foundation interaction system is modeled by the finite element method. Friction contact is considered in concrete slab-rockfill interface. Hydrodynamic pressure effects of the reservoir water are considered with fluid finite elements based on the Lagrangian approach In the nonlinear time-history analyses, Drucker-Prager model is used for concrete slab and multi-linear kinematic hardening model is utilized for rockfill zones and foundation soil. 1992 Erzincan earthquake with peak ground acceleration of 0.515g recorded near the dam site is used in analyses. All numerical applications are performed using ANSYS [26]. As a result, the variation of the face slab thickness clearly affects seismic performance of concrete slab. It is clearly distinguished from this study that the increase in the slab thickness results as an improvement in seismic performance of the face slab. Besides, hydrodynamic pressure decreases the seismic performance of the concrete slab. It is seen from the numerical results that increasing the slab thickness is effective and useful method to reduce the damages in concrete slab.

2. FORMULATION OF FLUID-STRUCTURE-FOUNDATION INTERACTION BY THE LAGRANGIAN APPROACH

The formulation of the fluid system is presented according to the Lagrangian approach [27]. In this approach, fluid is assumed to be linearly elastic, inviscid and irrotational. For a general two-dimensional fluid, stress-strain relationships can be written in matrix form as follows,

$$\begin{Bmatrix} P \\ P_z \end{Bmatrix} = \begin{bmatrix} C_{11} & 0 \\ 0 & C_{22} \end{bmatrix} \begin{Bmatrix} \varepsilon_v \\ w_z \end{Bmatrix} \tag{1}$$

where P, C_{11}, and εv are the pressures which are equal to mean stresses, the bulk modulus and the volumetric strains of the fluid, respectively. Since irrotationality of the fluid is considered like penalty methods [28], rotations and constraint parameters are included in the stress-strain equation "Eq. (1)" of the fluid. In this equation, P_z is the rotational stress; C_{22} is the constraint parameter and w_z is the rotation about the Cartesian axis z.

In this study, the equations of motion of the fluid system are obtained using energy principles. Using the finite element approximation, the total strain energy of the fluid system may be written as,

$$\pi_e = \frac{1}{2} \mathbf{U}_f^T \mathbf{K}_f \mathbf{U}_f \tag{2}$$

where $\mathbf{U}_f$ and $\mathbf{K}_f$ are the nodal displacement vector and the stiffness matrix of the fluid system, respectively. $\mathbf{K}_f$ is obtained by the sum of the stiffness matrices of the fluid elements in the following,

$$\mathbf{K}_f = \sum \mathbf{K}_f^e$$
$$\mathbf{K}_f^e = \int_V \mathbf{B}_f^{eT} \mathbf{C}_f \mathbf{B}_f^e dV^e \tag{3}$$

where $\mathbf{C}_f$ is the elasticity mat rix consisting of diagonal terms in "Eq. (1)". $\mathbf{B}_f^e$ is the strain-displacement matrix of the fluid element.

An important behaviour of fluid systems is the ability to displace without a change in volume. For reservoir and storage tanks, this movement is known as sloshing waves in which the displacement is in the vertical direction. The increase in the potential energy of the system due to the free surface motion can be written as,

$$\pi_s = \frac{1}{2} \mathbf{U}_{sf}^T \mathbf{S}_f \mathbf{U}_{sf} \tag{4}$$

where $\mathbf{U}_{sf}$ and $\mathbf{S}_f$ are the vertical nodal displacement vector and the stiffness matrix of the free surface of the fluid system, respectively. $\mathbf{S}_f$ is obtained by the sum of the stiffness matrices of the free surface fluid elements in the following,

$$\mathbf{S}_f = \sum \mathbf{S}_f^e$$
$$\mathbf{S}_f^e = \rho_f g \int_A \mathbf{h}_s^T \mathbf{h}_s dA^e \tag{5}$$

where $\mathbf{h}_s$ is the vector consisting of interpolation functions of the free surface fluid element. ρ_f and g are the mass density of the fluid and the acceleration due to gravity, respectively. Also, kinetic energy of the system can be written as,

$$T = \frac{1}{2} \dot{\mathbf{U}}_f^T \mathbf{M}_f \dot{\mathbf{U}}_f \tag{6}$$

where $\dot{\mathbf{U}}_f$ and $\mathbf{M}_f$ are the nodal velocity vector and the mass matrix of the fluid system, respectively. $\mathbf{M}_f$ is also obtained by the sum of the mass matrices of the fluid elements as following,

$$\mathbf{M}_f = \sum \mathbf{M}_f^e$$
$$\mathbf{M}_f^e = \rho_f \int_V \mathbf{H}^T \mathbf{H} dV^e \tag{7}$$

where H is the matrix consisting of interpolation functions of the fluid element. If "Eq. (2)", "(4)" and "(6)" are combined using the Lagrange's equation [29]; the following set of equations is obtained,

$$\mathbf{M}_f \ddot{\mathbf{U}}_f + \mathbf{K}_f^* \mathbf{U}_f = \mathbf{R}_f \tag{8}$$

where $\mathbf{K}_f^*$, $\ddot{\mathbf{U}}_f$ and $\mathbf{R}_f$ are the system stiffness matrix including the free surface stiffness, the nodal acceleration vector and time-varying nodal force vector for the fluid system, respectively. In the formation of the fluid element matrices, reduced integration orders are utilized [27].

The equations of motion of the fluid system, "Eq. (8)", have a similar form with those of the structure system. To obtain the coupled equations of the fluid-structure system, the determination of the interface condition is required. Because the fluid is assumed to be inviscid, only the displacement in the normal direction to the interface is continuous at the interface of the system. Assuming that the positive face is the structure and the negative face is the fluid, the boundary condition at the fluid-structure interface is,

$$U_n^- = U_n^+ \tag{9}$$

where U_n is the normal component of the interface displacement [30]. Using the interface condition, the equations of motion of the coupled system to ground motion including damping effects are given by,

$$\mathbf{M}_c\ddot{\mathbf{U}}_c + \mathbf{C}_c\dot{\mathbf{U}}_c + \mathbf{K}_c\mathbf{U}_c = \mathbf{R}_c \tag{10}$$

in which $\mathbf{M}_c$, $\mathbf{C}_c$ and $\mathbf{K}_c$ are the mass, damping and stiffness matrices for the coupled system, respectively. $\mathbf{U}_c$, $\dot{\mathbf{U}}_c$, $\ddot{\mathbf{U}}_c$ and $\mathbf{R}_c$ are the vectors of the displacements, velocities, accelerations and external loads of the coupled system, respectively.

3. STRUCTURAL PERFORMANCE AND DAMAGE CRITERIA FOR DAMS

Linear time-history analysis is used to formulate a systematic and rational methodology for qualitative estimate of the level of damage. In this analysis, deformations, stresses, and section forces are computed according to elastic stiffness characteristics of various components. When acceleration time-histories are used as the seismic input, both the magnitudes and time-varying characteristics of the seismic response is calculated by the linear time-history analysis. A systematic interpretation and evaluation of these results in terms of the demand-capacity ratios (D/C), cumulative inelastic duration, spatial extent of overstressed regions, and consideration of possible modes of failure form the basis for approximation and appraisal of probable level of damage. The damage for structural performance comes to mean to cracking of the concrete, opening of construction joints and yielding of the reinforcing steel. If the estimated level of damage falls below the acceptance curve, where D/C is between 1 and 2, for a particular type of structure, the damage is considered to be low and the linear time-history analysis will be adequate. Otherwise the damage is considered to be severe, in which case a nonlinear time-history analysis would be required to estimate damage more truly [31].

The maximum permitted demand-capacity ratio for linear analysis of dam is 2 [31]. A demand-capacity ratio of 2 allows stresses up to twice the static tensile strength of the concrete or to the level of dynamic apparent tensile strength. The cumulative duration beyond a certain level of demand-capacity ratio is obtained by multiplying number of stress values exceeding that level by the time-step of the time-history analysis. The cumulative duration in Figure 1 refers to the total duration of all stress excursions beyond a certain level of demand-capacity ratio.

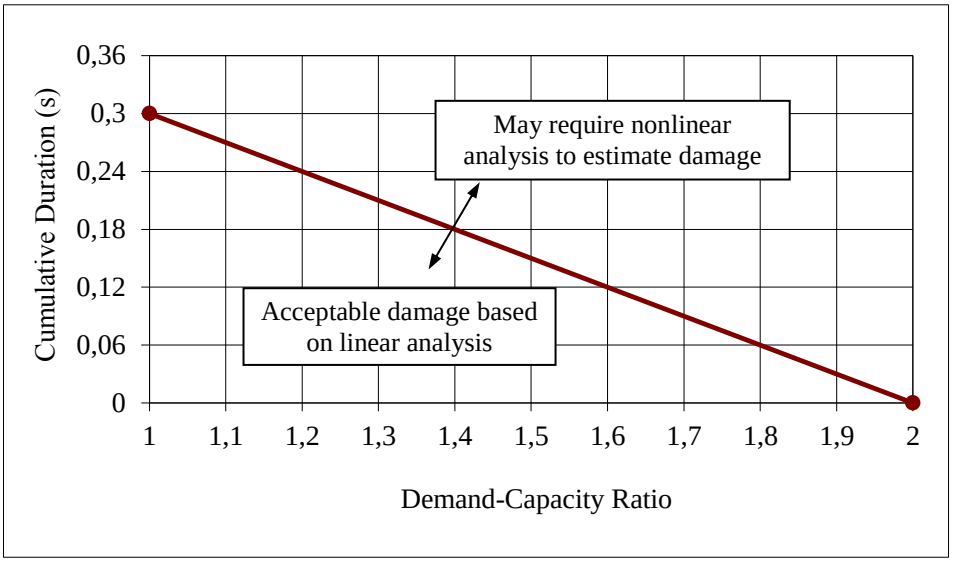

Figure 1. Assumed performance curve for linear elastic analysis [31].

4. THE DRUCKER-PRAGER MODEL

There are many criteria for determination of yield surface or yield function of materials. The Drucker-Prager criterion is widely used for frictional materials such as rock and concrete. Drucker and Prager [32] obtained a convenient yield function to determine elasto-plastic behaviour of concrete smoothing Mohr-Coulomb criterion (Figure 2) [33]. This function is defined as:

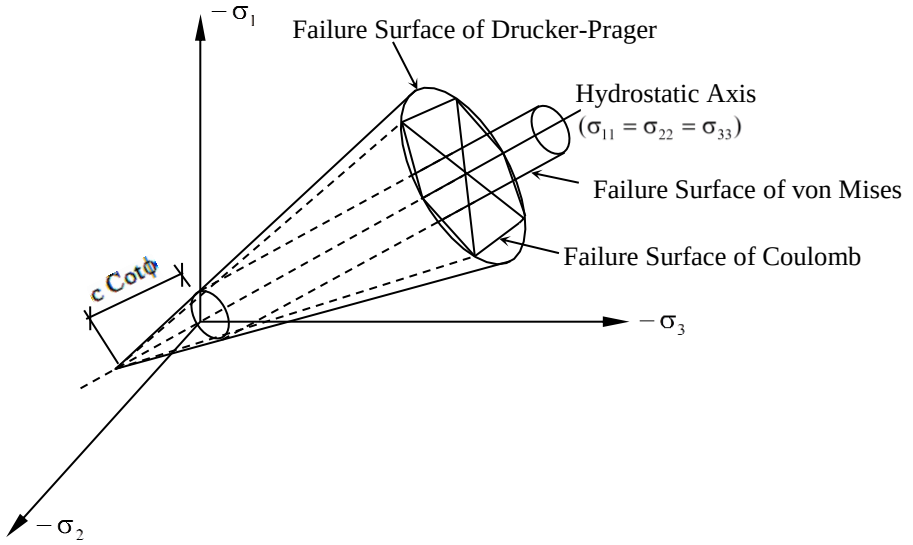

Figure 2. Failure criteria for Coulomb, Drucker-Prager and von Mises [33].

$$f = \alpha I_1 + \sqrt{J_2} - k \tag{11}$$

where α and k are constants which depend on cohesion (c) and angle of internal friction (ϕ) of the material given by

$$\alpha = \frac{2\ \mathrm{Sin}\varphi}{\sqrt{3}\ (3 - \mathrm{Sin}\varphi)}$$
$$k = \frac{6c\ \mathrm{Cos}\varphi}{\sqrt{3}\ (3 - \mathrm{Sin}\varphi)} \tag{12}$$

In Eq. (11), I_1 is the first invariant of stress tensor (σ_{ij}) formulated as follows,

$$I_1 = \sigma_{11} + \sigma_{22} + \sigma_{33} \tag{13}$$

and J_2 is the second invariant of deviatoric stress tensor (s_{ij}) given by,

$$J_2 = \frac{1}{2} s_{ij} s_{ij} \tag{14}$$

where, s_{ij} is the deviatoric stresses as yielded below.

$$s_{ij} = \sigma_{ij} - \delta_{ij}\sigma_m \qquad (i, j = 1,2,3) \tag{15}$$

In Eq. (15), δ_{ij} is the kronecker delta, which is equal to 1 for i=j; 0 for i≠j, and σ_m is the mean stress and obtained as follows,

$$\sigma_m = \frac{I_1}{3} = \frac{\sigma_{ii}}{3} \tag{16}$$

If the terms in Eq. (15) are obtained by Eq. (16) and replaced in Eq. (14), the second invariant of the deviatoric stress tensor can be obtained as follows:

$$J_2 = \frac{1}{6}\left[(\sigma_{11} - \sigma_{22})^2 + (\sigma_{22} - \sigma_{33})^2 + (\sigma_{33} - \sigma_{11})^2\right] + {\sigma_{12}}^2 + {\sigma_{13}}^2 + {\sigma_{23}}^2 \tag{17}$$

5. TORUL DAM

Torul CFR Dam is located on Harsit River and approximately 14 km northwest of Torul, Gumushane (Figure 3). Torul Dam was completed in 2007 by General Directorate of State Hydraulic Works [34]. The main objective of the reservoir is power generation. The volume of the dam body is 4.6 hm^3 and the lake area of the dam at the normal water level is 3.62 km^2. The annual total power generation capacity is 322.28 GW. The length of the dam crest is 320 m and its wide is 12 m, and the maximum height and base width are 142 m and 420 m, respectively. The two-dimensional largest cross section and the dimensions of the dam are shown in Figure 4.

5.1. Material Properties

The Torul dam body consists of concrete face slab and five rockfill zones: 2A, 3A, 3B, 3C, 3D, respectively, from upstream toward downstream. These rockfill zones are arranged from thin granules to thick particles in upstream-downstream direction. Foundation soil is formed of

limestone (below) and volcanic tufa (upper) as two layers [34]. The material properties of the dam body, foundation soil and the reservoir water used in linear and nonlinear analyses are submitted in Table 1. The concrete slab has high resistance to water penetration. In addition, tensile and compression strengths of the concrete are 1.6 MPa and 20 MPa respectively [35]. Besides, the cohesion and angle of internal friction of the concrete is 2500 kPa and 30°, respectively. The bulk modulus of reservoir water and density are assumed as 2.07 MPa and 1000 kg/m^3.

a) Upstream face

b) Downstream face

Figure 3. View of the Torul CFR dam [36].

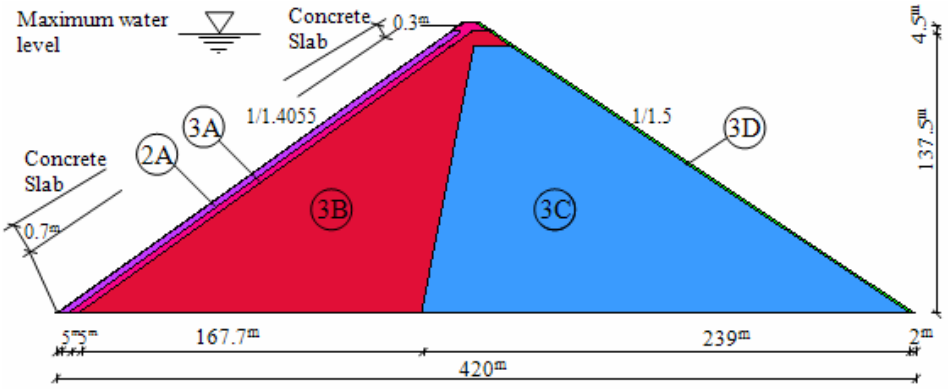

Figure 4. The largest cross-section of Torul dam [36].

Table 1. Material properties.

Material	Material Properties				
	Modulus of Elasticity $\times 10^7$ kPa	Poisson's Ratio	Mass per unit Vol. kg/m^3	Cohesion kPa	Angle of internal friction
Concrete	2.800	0.20	2395.5	2500	30
2A (sifted rock or alluvium)	0.040	0.36	1880.0	-	-
3A (filling with selected rock)	0.030	0.36	1870.0	-	-
3B (filling with quarry rock)	0.025	0.32	1850.0	-	-
3C (filling with quarry rock)	0.020	0.32	1850.0	-	-
3D (filling with selected rock)	0.040	0.26	1800.0	-	-
Foundation Soil (volcanic tufa)	1.036	0.17	-	-	-
Foundation Soil (limestone)	1.206	0.18	-	-	-

5.2. Finite Element Model

The two-dimensional dam-foundation-reservoir finite element model used in analyses is shown in Figure 5. In this model, dam body has 592 solid finite elements, foundation soil has 656 solid finite elements, reservoir water has 495 fluid finite elements and 16 interface elements are defined between concrete slab and rockfill. The damping ratio of 5% is assumed in all finite element analyses for dam and reservoir water. Massless foundation is used in time-history analyses. Coupling length is chosen as 1 mm at the reservoir-dam and reservoir-foundation interface and 50 numbers of couplings are defined in dam-reservoir-foundation model. The main objective of the couplings is to hold equal the displacements between two reciprocal nodes in normal direction to the interface. The length for both reservoir and foundation soil in the upstream direction is taken into consideration as three times of the dam height. Besides, the total height of the foundation layers and soil length at the downstream direction are taken into account as much as the dam height.

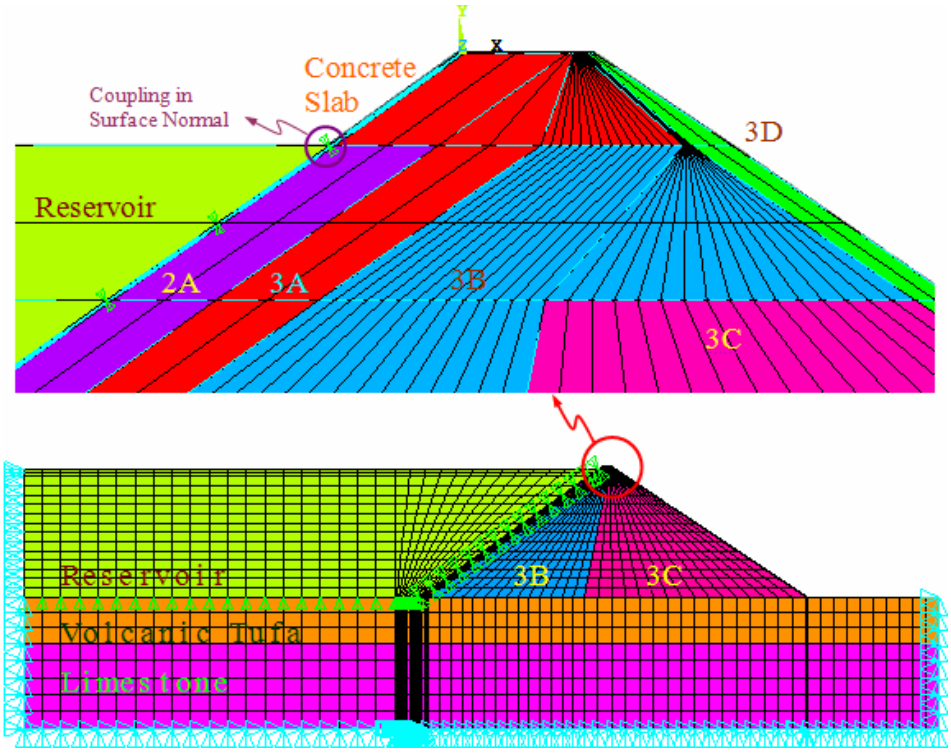

Figure 5. The two-dimensional finite element model of Torul Dam [36].

5.3. Concrete Slab - Rockfill Interface

The earthquake response of concrete slab is mostly depended upon its conjunction to rockfill. The joint can be modelled as welded contact and friction contact (Figure 6). Actually, concrete slab does not directly contact with the rockfill. According to this observation, the use of interface element in finite element analysis can provide more realistic results. The special material constituting this element allows through-thickness and transverse shear deformation. Concrete slab may slide over the face of rockfill and also leave and close to rockfill by using this element. In this study, concrete slab and rockfill are assumed as independent deformable bodies by using interface elements. The interface element used in this study has four node and two integration points. The transverse shear stiffness of the interface is assumed as 2000 kPa/m.

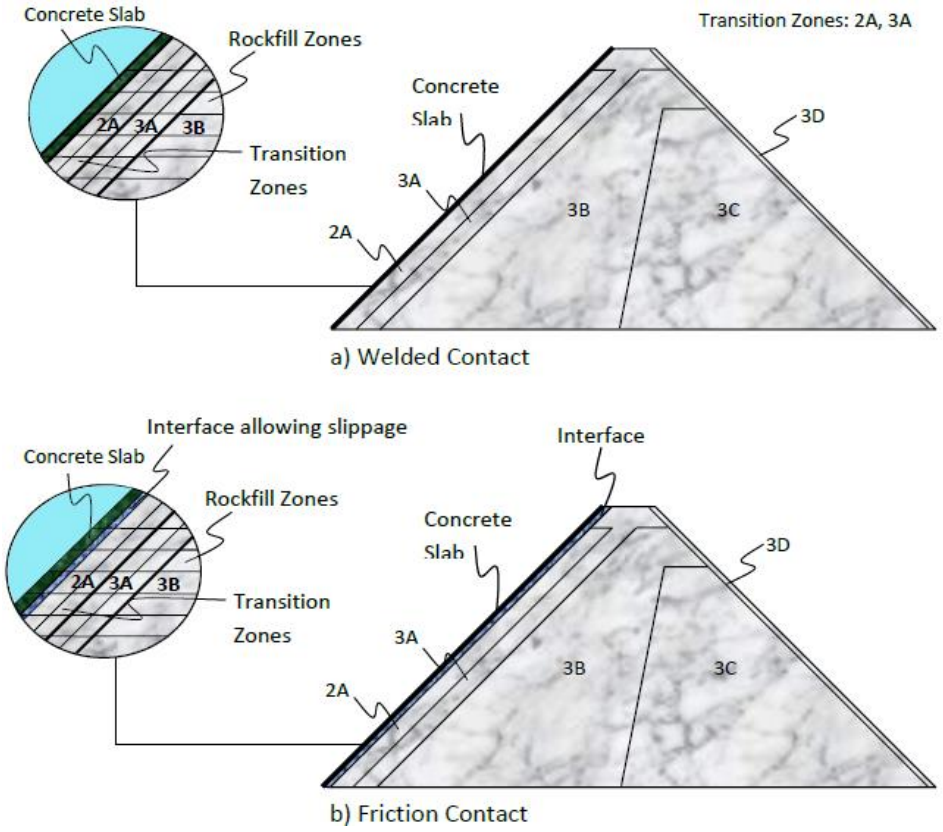

Figure 6. Connection types in concrete slab-rockfill interface.

5.4. Concrete Face Slab Thickness

Performance of concrete face slab thickness is one of the major issues of the researchers. Many formulations have been developed and used in design of CFR dams. Face slab thickness of Torul CFR Dam is 0.3 m at the top and reaches linearly increasing to 0.7 m at the bottom of concrete slab. In this study, slab thickness is assumed to be constant at the top of the dam as 0.3 m. However, slab thickness of CFR dams has been determined using different functions usually depending on dam height [37]. The face slab thickness functions used in this study are given in Table 2.

Table 2. Various thickness functions of concrete slab on CFR dams [37].

Functions of Slab Thickness	Slab Thickness (m)		Some Referenced CFR Dams – Year Completed
	Top	Bottom	
t = 0.3	0.3	0.3	Chusong-1999, Douyan-1995, Hengshan-1992 etc...
t = 0.3 + 0.002H	0.3	0.584	Baiyun-1998, Da'ao-1999, Tianhuagping-1997 etc…
t = 0.3 + 0.003H	0.3	0.726	Baixi- 2001, Tankeng-2005, Xiaoshan-1997 etc…
t = 0.3 + 0.004H	0.3	0.868	Gouhou-1989
t = 0.3 – 1.1	0.3	1.1	Jiangpinghe- (221m)

H→ Dam height.

6. PERFORMANCE ANALYSIS OF TORUL CFR DAM

Seismic performance analysis of Torul CFR Dam is evaluated for the 1992 Erzincan earthquake record with pga of 0.515g shown in Figure 7 [38]. The effect of face slab thickness on seismic performance of concrete slab on CFR dam forms the basis of this study. Performance analyses are performed using finite element method. Numerical analyses are carried out for empty and full reservoir cases of the dam. Firstly, linear time-history analyses are performed to assess the damage to be occurred in the concrete whether it is acceptable or not by considering the demand-capacity ratio interval between 1 and 2. The demand-capacity ratios are considered for the principle tensile stresses occurred in the concrete slab during earthquake. The variation of principle tensile stresses occurred in face slab is given in Figures 8 and 9 which are shown according to face slab thickness at foundation level. As seen from Figures 8 and 9, maximum principal stresses exceed the tensile strength of the concrete too many times for all face slab thicknesses and each case of the reservoir. As the face slab thickness increases, the maximum principle stress occurred in concrete slab decreases in both case of the dam reservoir. At this point of the study, it should clearly be clarified that, there is a decrease about 1.6 MPa in the concrete slab of the dam that have 1.1 m thickness at foundation as compared to one which have constant thickness of 0.3 m.

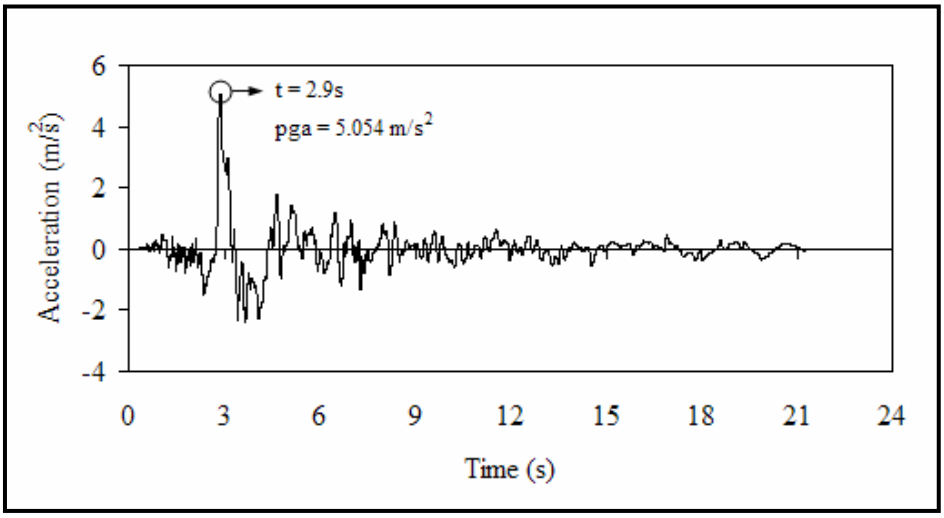

Figure 7. 1992 Erzincan earthquake record with pga of 0.515 g [38].

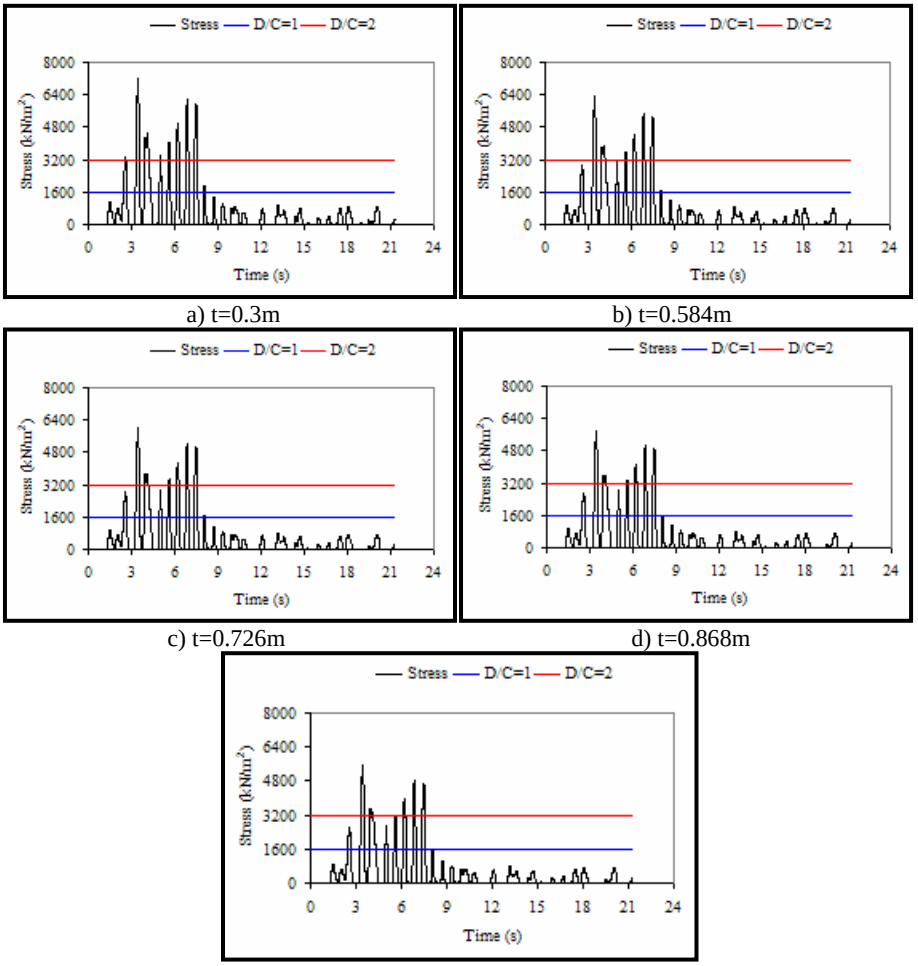

a) t=0.3m b) t=0.584m

c) t=0.726m d) t=0.868m

e) t=1.1m

Figure 8. Principle tensile stress cycles for linear analyses in empty reservoir case.

Earthquake performance curves are drawn for linear time-history analyses. These curves are shown in

Figure 10 according to face slab thickness at foundation level of the dam. Seismic performance evaluation of the concrete slab is realized for both reservoir cases. As seen from

Figure 10, seismic performance of the concrete slab is clearly improved by increasing face slab thickness. In addition, hydrodynamic pressure decreases the seismic performance of the concrete slab. According to performance analyses, CFR dam, which has the concrete slab with constant slab thickness of 0.3 m, shows the lowest seismic performance. Linear analyses obviously indicate that inevitable cracks will occur in concrete slab. Therefore, seismic performance assessment of the dam requires nonlinear analysis to obtain more rational results.

The principle tensile stress cycles attained from nonlinear analyses are shown in Figures 11 and 12 for both reservoir cases. According to nonlinear analyses, principle tensile stresses are relatively close each other for different slab thicknesses. However, if linear analysis results are compared to nonlinear analysis ones, there is an obvious decrease in principle tensile stresses.

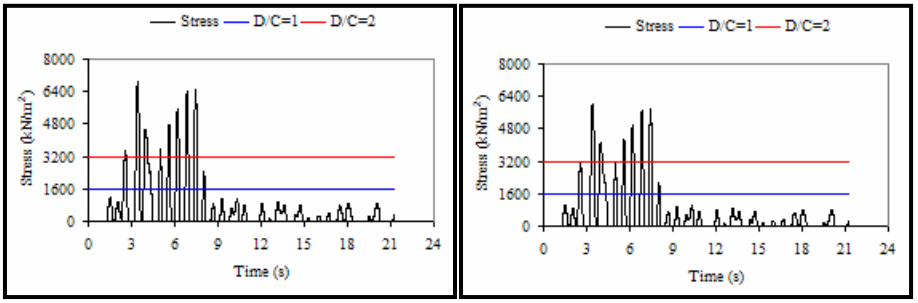

a) t=0.3m b) t=0.584m

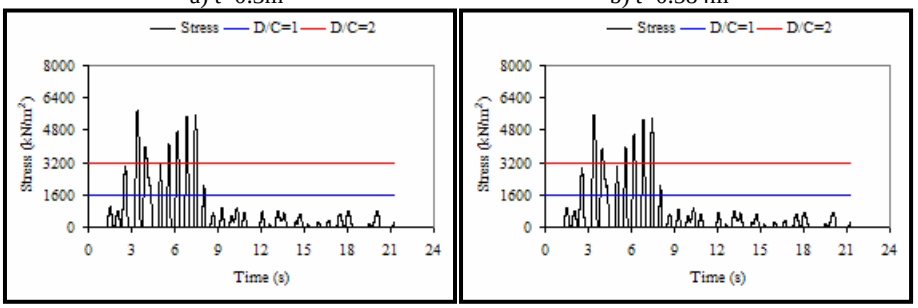

c) t=0.726m d) t=0.868m

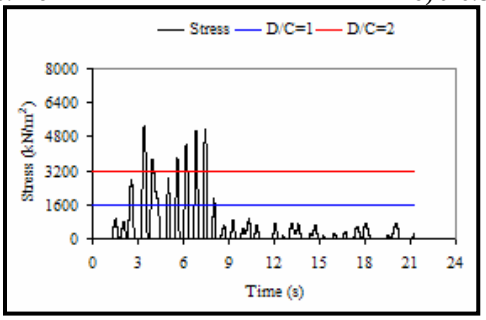

e) t=1.1m

Figure 9. Principle tensile stress cycles for linear analyses in full reservoir case.

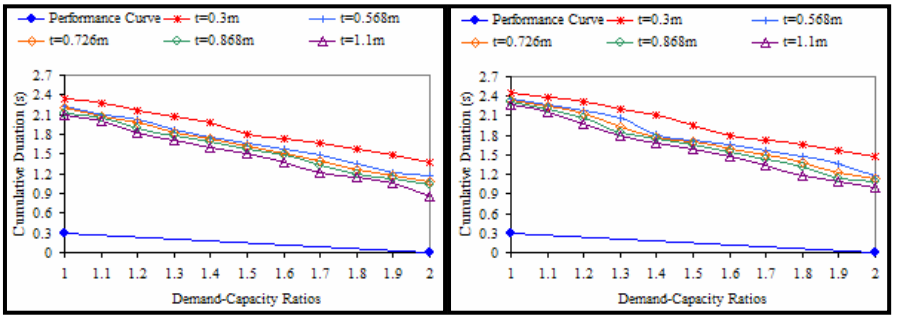

a) Empty reservoir case b) Full reservoir case

Figure 10. Performance curves according to linear analyses.

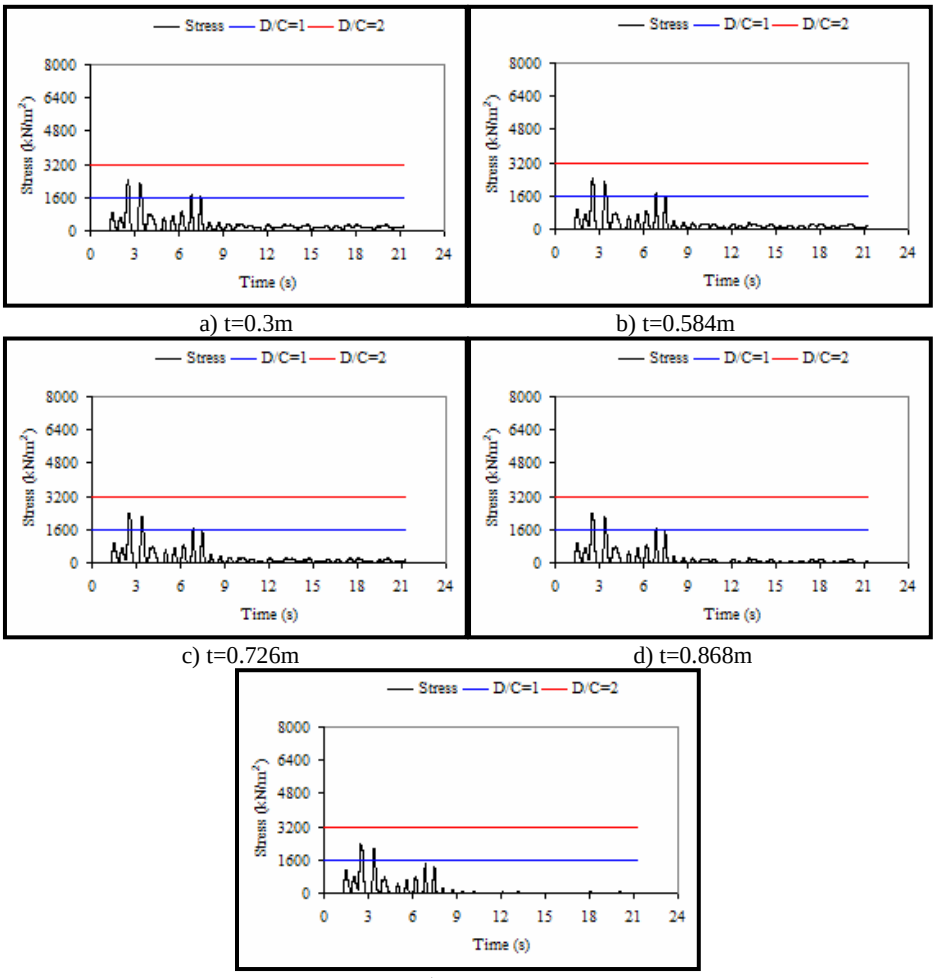

a) t=0.3m b) t=0.584m

c) t=0.726m d) t=0.868m

e) t=1.1m

Figure 11. Principle tensile stress cycles for nonlinear analyses in empty reservoir case.

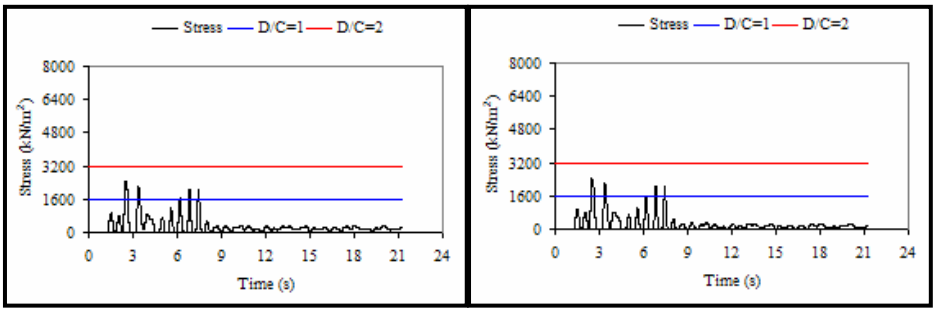

a) t=0.3m b) t=0.584m

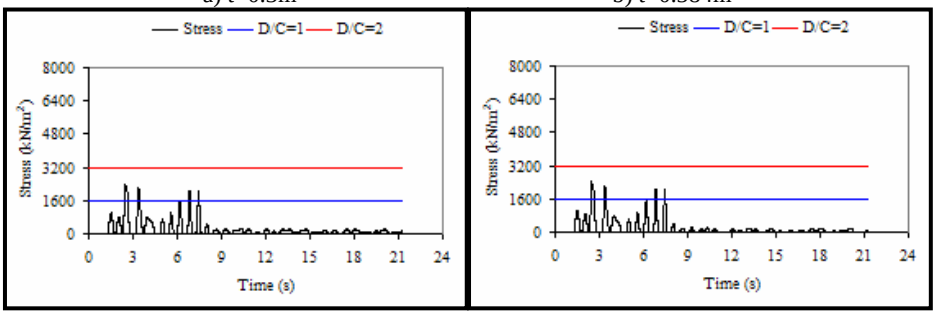

c) t=0.726m d) t=0.868m

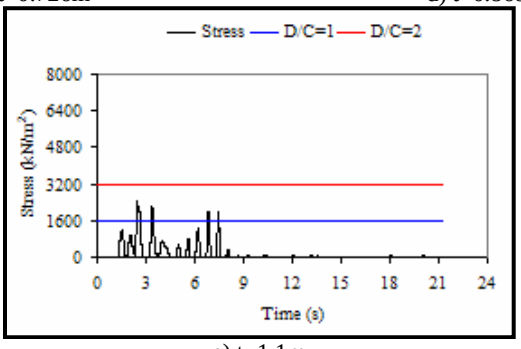

e) t=1.1m

Figure 12. Principle tensile stress cycles for nonlinear analyses in full reservoir case.

In order to obtain the seismic performance evaluation of the concrete slab more obvious, performance curves obtained from nonlinear analyses are drawn in Figure 13.

Although crack formation in concrete seems evidently lower, damage because of high tensile stress repetition will probably occur. In both case of the reservoir, damage forming for the values of D/C greater than 1.35 does not exist. For the lower demand-capacity ratios cracks may probably occur but as the thickness of the slab increases, concrete slab will be less compelled. In addition, hydrodynamic pressure decreases seismic performance of the slab. Therefore, damage level increases in the existence of hydrodynamic pressure.

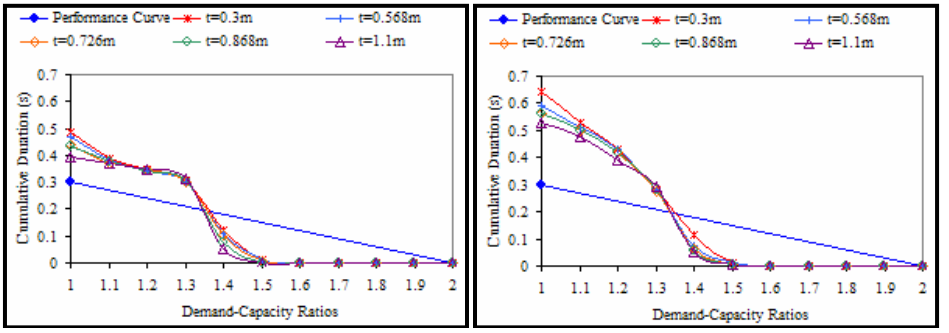

a) Empty reservoir case b) Full reservoir case

Figure 13. Performance curves according to nonlinear analyses.

7. CONCLUSIONS

Seismic performance of the concrete slab on CFR dam is investigated. The effect of the concrete slab thickness on seismic performance of the face slab forms a basis of this research. In the scope of the study, five different slab thicknesses derived using the formulations received from the literature are used.

This study reveals that geometrical properties of the concrete slab on CFR dam are quite effective on seismic performance of the concrete slab. In addition to this, hydrodynamic pressure has also reducing effect on the seismic performance of the concrete slab. In addition, materially nonlinear analyses are resulted as higher earthquake performance for concrete slab.

CFR dams located in regions that have seismically high risks may be exposed to strong ground motions. Therefore, selection of the concrete slab thickness seems as important as the material properties of the concrete and earthquake record. However, friction contact in concrete slab-rockfill interface should also been taken into consideration in design stage. Rockfill dams actually can not behave linear elastic; hence nonlinear analyses should be performed to determine realistic performance of dam.

REFERENCES

[1] Seed, H.B., Seed, R.B., Lai, S.S., (1985) Khamenehpour, B. Seismic Design of Concrete Faced Rockfill Dams, *Proceedings of the Symposium on Concrete Face Rockfill Dams - Design, Construction and Performance, ASCE*, New York, 459-478.

[2] Uddin, N., (1999) A Dynamic analysis Procedure for Concrete-Faced Rockfill Dams Subjected to Strong Seismic Excitation, *Computers and Structures* 113(1-3), 409-421.

[3] Guros, F.B., Thiers, G.R., Wathen, T.R., Buckles, C.E., (1984) Seismic Design of Concrete-Faced Rockfill Dams, *Proceedings of the 8th World Conference on Earthquake Engineering*, San Francisco: Prentice-Hall, Englewood Cliffs, NJ, 3: 317-323.

[4] Arrau, L., Ibarra, I., Noguera, G., (1985) Performance of Cogoti Dam Under Seismic Loading, *Concrete Face Rockfill Dams-Design, Construction and Performance, ASCE*, New York, 1-14.

[5] Bureau, G., Volpe, R.L., Roth, W., Udaka, T., (1985) Seismic Analysis of Concrete Face Rockfill Dams, *Proceedings of the Symposium on Concrete Face Rockfill Dams – Design, Construction and Performance, ASCE*, Detroit, Michigan, New York, 479-508.

[6] Priscu, R., Popovici, A., Stematiu, D., Stere, C., (1985) Earthquake Engineering for Large Dams, Editura Academiei: Bucuresti and John Wiley & Sons, New York.

[7] Sherard, J.L., Cooke, J. B. (1987) Concrete-face rockfill dam – I. Assessment, and II. Design, *Journal of Geotechnical Engineering* 113(10), 1096-1132.
[8] Gazetas, G. and Dakoulas, P. (1992) Seismic analysis and design of rockfill dams – State of the Art. *Soil Dynamics and Earthquake Engineering* 11: 27-61.
[9] Chrzanowski, A.S., Massiéra, M. (2006) Relation Between Monitoring and Design Aspects of Large Earth Dams, *3rd IAG / 12th FIG Symposium*, Baden.
[10] Westergaard, H.M., (1933) Water Pressures on Dams During Earthquakes. *Transactions, ASCE* 98, 418-433.
[11] Zangar, C.N., Haefei, R.J., (1952) Electric Analog Indicates Effects of Horizontal Earthquake Shock on Dams, *Civil Engineering*, 54-55.
[12] Zienkiewicz, O.C., (1963) Nath, B. Earthquake Hydrodynamic Pressures on Arch Dams-an Electric Analogue Solution, *Proceedings of International Civil Engineering Congress*, 25, 165-176.
[13] Chopra, A.K., (1968) Earthquake Behavior of Reservoir-Dam Systems, *Journal of Engineering Mechanics Division* 94, 1475-1500.
[14] Finn, W.D.L., Varoglu, E., (1973) Dynamics of Gravity Dam-Reservoir Systems, *Computers and Structures* 3, 913-924.
[15] Saini, S.S., Bettess, P., Zienkiewicz, O.C., (1978) Coupled Hydrodynamic Response of Concrete Gravity Dams Using Finite and Infinite Elements, *Earthquake Engineering and Structural Dynamics* 6, 363-374.
[16] Chopra, A.K. and Chakrabarti, P., (1981) Earthquake Analysis of Concrete Gravity Dams Including Dam-Water-Foundation Rock Interaction, *Earthquake Engineering and Structural Dynamics* 9, 363-383.
[17] Greeves, E.J., Dumanoglu, A.A., (1989) The Implementation of an Efficient Computer Analysis for Fluid-Structure Interaction Using the Eulerian Approach within SAP-IV. Department of Civil Engineering, University of Bristol, Bristol.
[18] Singhal, A.C., (1991) Comparison of Computer Codes for Seismic Analysis of Dams. *Computers and Structures* 38, 107-112.
[19] Calayir, Y., Dumanoglu, A.A., Bayraktar, A., (1996) Earthquake Analysis of Gravity Dam–Reservoir Systems Using the Eulerian and Lagrangian Approaches, *Computers and Structures* 59, 877-890.
[20] Bayraktar, A., Dumanoglu, A.A., Calayır, Y., (1996) Asynchronous Dynamic Analysis of Dam-Reservoir-Foundation Systems by the Lagrangian Approach, *Computers and Structures* 58, 925-935.
[21] Bayraktar, A., Altunışık, A.C., Sevim, B., Kartal, M.E., Türker, T., (2008) Near-Fault Ground Motion Effects on the Nonlinear Response of Dam-Reservoir-Foundation Systems, *Structural Engineering and Mechanics* 28(4), 411-442.
[22] Bayraktar, A., Sevim, B., Altunışık, A.C., Türker, T., Kartal, M.E., Akköse, M., Bilici, Y., (2009) Comparison of Near and Far Fault Ground Motion Effects on the Seismic Performance Evaluation of Dam-Reservoir-Foundation Systems, *International Water Power & Dam Construction (Dam Engineering)* 19(3), 1-39.
[23] Bayraktar, A., Kartal, M.E., Basaga, H.B., (2009) Reservoir Water Effects on Earthquake Performance Evaluation of Torul Concrete-Faced Rockfill Dam, *Water Science and Engineering* 2(1), 43-57.
[24] Kartal, M.E., (2018) Investigation of the Deformations in a Concrete Faced Rockfill Dam During Strong Ground Motion, *Sigma Journal of Engineering and Natural Sciences* 36(1), 207-230.
[25] Kartal, M.E., (2019) Earthquake Performance of Concrete Slab on Concrete Faced Rockfill Dam Including Hydrodynamic Effects, *Sigma Journal of Engineering and Natural Sciences* 37(2), 641-674.
[26] ANSYS 15.0, (2015) Swanson Analysis Systems Inc., Houston PA, USA.

[27] Wilson, E.L., Khalvati, M., (1983) Finite Elements for the Dynamic Analysis of Fluid-Solid Systems, *International Journal for Numerical Methods in Engineering* 19, 1657-1668.
[28] Zienkiewicz, O.C., Taylor, R.L., (1989) The Finite Element Method. *Mc Graw-Hill*.
[29] Clough, R.W. and Penzien, J. (1993) Dynamics of Structures, 2nd edition, *McGraw-Hill*, Singapore.
[30] Akkas, N., Akay, H.U., Yılmaz, C., (1979) Applicability of General-Purpose Finite Element Programs in Solid-Fluid Interaction Problems, *Computers and Structures* 10, 773-783.
[31] Ghanaat, Y., (2002) Seismic Performance and Damage Criteria for Concrete Dams, *Proceedings of the 3rd US-Japan Workshop on Advanced Research on Earthquake Engineering for Dams*, San Diego, California.
[32] Drucker DC, Prager W. Soil Mechanics and Plastic Analysis of Limit Design, Quart. Applied Mathematics, 1952;10(2).
[33] Chen WF, Mizuno E. Nonlinear analysis in soil mechanics, Elsevier, New York, 1990.
[34] DSI, (2019) General Directorate of State Hydraulic Works, http://www.dsi.gov.tr/english/.
[35] TS 500, (2000) Turkish Standard, Requirements for Design and Construction of Reinforced Concrete Structures.
[36] Kartal, M.E., (2010) Reliability Analysis of Concrete-Faced Rockfill Dams, Ph.D. Thesis, *Graduate School of Natural and Applied Sciences, Karadeniz Technical University*, Trabzon Turkey.
[37] Qian, C., (2005) Recent Development of CFRD in China, *Proceedings of Symposium on 20 years for Chinese CFRD Construction*, Yichang, China, 8-15.
[38] PEER, (2015) Pacific Earthquake Engineering Research Centre, http://peer.berkeley.edu /smcat/data.